Available online at www.sciencedirect.com
ScienceDirect
Journal of the European Ceramic Society 27 (2007) 2347–2354
www.elsevier.com/locate/jeurceramsoc

Comparison of fracture resistance as measured by the indentation fracture method and fracture toughness determined by the single-edge-precracked beam technique using silicon nitrides with different microstructures

Hiroyuki Miyazaki *, Hideki Hyuga, Kiyoshi Hirao, Tatsuki Ohji

National Institute of Advanced Industrial Science and Technology (AIST), Anagahora 2266-98, Shimo-shidami, Moriyama-ku, Nagoya 463-8560, Japan

Received 9 June 2006; received in revised form 8 September 2006; accepted 16 September 2006
Available online 1 November 2006

Abstract

Because of the industrial need for an assessment of fracture resistance, K_R from small ceramic parts, K_R of Si_3N_4 ceramics has been measured by the indentation fracture (IF) method using representative formulae to evaluate the compatibility with the fracture toughness, K_{Ic} determined from the single-edge-precracked beam (SEPB) technique. K_R of the fine Si_3N_4 showed little dependence on the crack length, whereas the samples with coarse microstructures exhibited a rising *R*-curve behavior. The IF equation which gave the nearest value to K_{Ic} from SEPB was different depending on the microstructures. The assessment of fracture resistance with Miyoshi's equation was considered to be preferable for the flat *R*-curve behavior. By contrast, in the case of the rising *R*-curve behavior, it was revealed that the relationship between the IF and SEPB values was difficult to explain unless the effective crack extension against K_{Ic} for SEPB was clarified.

Keywords: Si_3N_4; Toughness and toughening; Indentation fracture

1. Introduction

The indentation fracture (IF) technique, proposed by Lawn et al.,[1] has been widely used for estimating the fracture resistance of brittle materials, particularly glasses and ceramics. Compared with conventional measurement techniques such as single-edge-precracked beam (SEPB)[2,3] and chevron-notched beam, this technique is particularly useful when the sizes of available specimens are limited. Silicon nitrides are considered as promising structural materials for usage in severe environments and many attempts have been conducted to improve their mechanical properties through microstructural control. One of the successful applications of the developed Si_3N_4 is tribological components in corrosive surroundings such as bearings for hard disks and mechanical seals, and the market has been expanding. For such applications, it is very important to assess the fracture resistance of real parts themselves. However, tribological parts such as bearings generally have limited sizes, and in that case, the IF method is the most useful technique for fracture resistance evaluation.

Many formulae have been proposed to figure out the fracture resistance from the observed as-indented crack length,[3–8] each leading to different values.[9–11] Consequently, the indentation technique was used only for comparison.[12,13] From an industrial point of view, one of the solutions to the market's demand for fracture resistance assessment of small parts is to choose the preferable IF equation which gives a comparable value to the fracture toughness from SEPB tests since the SEPB technique is standardized and is used widely in the engineering field.[3] It is also important to verify the effective range of the selected IF equation since a variety of Si_3N_4 with superior properties have been developed in the last decade through microstructural design.[13] In this paper, Si_3N_4 with various microstructures from fine to coarse and elongated have been prepared by controlling the amounts of sintering additives and sintering times, and their fracture resistance was determined by the IF method with various indentation loads using four representative equations: Miyoshi, Sagawa and Sasa's equation (hereafter Miyoshi's equation),[4] Anstis, Chantikul, Lawn and Marshall's one (hereafter Anstis's equation),[6] Ramachandran and Shetty's

* Corresponding author. Tel.: +81 52 736 7486; fax: +81 52 736 7405.
E-mail address: h-miyazaki@aist.go.jp (H. Miyazaki).

0955-2219/$ – see front matter © 2006 Elsevier Ltd. All rights reserved.
doi:10.1016/j.jeurceramsoc.2006.09.002

one (hereafter Ramachandran's equation)[7] and Niihara, Morena and Hasselman's one for median cracks (hereafter Niihara's equation).[5] These four equations possess almost the same form but differ in some adjustable constants.

The obtained results were compared with those determined by SEPB method,[3] and discussed in conjunction with their *R*-curve behavior which was obtained from the data of IF, as well as the data attained by the indentation-strength-in-bending (ISB) method.[14]

2. Experimental procedure

2.1. Materials

The starting powders used in this study were α-Si_3N_4 powder (SN-E10, Ube Industries Ltd., Japan), Al_2O_3 (AKP-50, Sumitomo Chemical Ltd., Japan) and Y_2O_3 (Shin-Etsu Rare Earth Ltd., Japan). Two types of compositions were prepared with these powders, one with 1 wt% Al_2O_3 and 1 wt% Y_2O_3 (hereafter 1A1Y) and the other with 5 wt% Al_2O_3 and 5 wt% Y_2O_3 (hereafter 5A5Y). They were mixed in ethanol using nylon-coated iron balls and a nylon pot for 24 h. The slurry was dried, and then passed through 125 mesh sieve. The 1A1Y powder was hot-pressed at 1950 °C for 2 h with an applied pressure of 40 MPa in a 0.9 MPa N_2 atmosphere. In order to synthesize two kinds of samples from 5A5Y powder, the same fabrication procedure was employed except the sintering time was 2 and 8 h.

Densities of the sintered bodies were measured using the Archimedes technique. Relative densities were calculated on the assumption that the density of the grain boundary phase was almost the same as that of the composites of alumina (3.99 g/cm^3) and yttria (4.84 g/cm^3). The machined samples were polished and plasma etched in CF_4 gas before microstructural observation by scanning electron microscopy (SEM). The diameter of each grain was determined from the shortest grain diagonal in two-dimensional images with magnifications of 10k (1A1Y) and 5k (5A5Y). In the micrographs with the high magnification such as 5 and 10k, coarse and elongated grains occasionally appeared and most of them were interrupted by the frame of the pictures. In order to capture the whole features of these grains and count their frequency statistically, only the coarse grains (major axis > ∼8 μm) were selected from the micrographs with the lower magnification of 1k. Median grain diameters were attained from their cumulative distributions (sample size, *N*, were ∼700 for 1A1Y, ∼1100 for 5A5Y (1950 °C/2 h) and ∼450 for 5A5Y (1950 °C/8 h)). Aspect ratios of the grains in the 5 and 10k magnification images were estimated from the mean value of the 10% highest observed aspect ratios.[15] Aspect ratios of the coarse grains selected from the micrographs at a magnification of 1k were calculated by the same procedure as mentioned above.

2.2. Mechanical test procedure

Young's modulus was measured by the ultrasonic pulse echo method. Fracture toughness, K_{Ic}, was determined by the SEPB method with a span of 30 or 16 mm and a pop-in crack depth of about 2 mm ($N = 5$).[3] The fracture toughness measurement was carried out so that tensile stress during measurements was perpendicular to the hot-pressing direction. Vickers indentations were made on the polished surface perpendicular to the hot-pressing axis. The range of indentation load was from 49 to 490 N for the as-indented crack length measurements. The length of the impression diagonals and surface cracks were measured with a measuring microscope immediately after the indentation. Only indentations whose four primary cracks emanated straight forward from each corner were accepted. Indentations whose horizontal crack length differed by more than ∼10% from the vertical one were rejected as well as those with badly split cracks or with gross chipping. In most cases, nearly all the indentations were acceptable and the numbers of the indentations, *N* used for the calculation of K_R at each load was 6–9. When the 1A1Y sample was indented at the load of 490 N, however, some of the indentations experienced serious chipping, which reduced the number to 5. In the case of 5A5Y (1950 °C/8 h) at 49 and 490 N, $N = 4$ and 5, respectively, because almost half of indentations had unacceptable crack morphology.

The indentation load ranges for the indentation-strength measurements were from 49 to 294 N for 1A1Y and 5A5Y (1950 °C/2 h) and from 9.8 to 294 N for 5A5Y (1950 °C/8 h) ($N = 1$–2). The lengths of the impression diagonals and surface cracks were measured immediately after the indentation. For the indentation-strength measurement specimens, silicon oil was placed on the impression immediately after the indentation to avoid moisture-assisted subcritical growth of the as-indented cracks. Three-point flexural tests with a lower span of 16 mm were conducted at a crosshead speed of 0.02 mm/min.

2.3. Determination of fracture resistance (R-curves)

The fracture resistance, K_R, can be determined from the as-indented crack lengths as follows:

$$K_R = \xi \left(\frac{E}{H}\right)^n P c_0^{-3/2} \quad (1)$$

where ξ is the material-independent constant, n the dimensionless constant for Vickers produced radial cracks, E the Young's modulus, H the Vickers hardness for the Miyoshi,[4] Niihara[5] and Ramachandran[7] equations, whereas H is the mean contact pressure (load over projected area) in the Anstis formula.[6] P is the indentation load and c_0 is the half-length of as-indented surface crack length. Although the dependence of H on P was negligible in the load range investigated, H was calculated for each indentation and substituted into Eq. (1) to calculate K_R for each indentation. The values for n in those equations presented by Miyoshi, Anstis and Ramachandran are equal and $n = 1/2$ since these equations were based on the analysis of Lawn et al.[1] The difference among the three equations lies in the value of ξ: 0.018 for the Miyoshi's equation, 0.016 for Anstis's one and 0.023 for Ramachandran's one. Miyoshi et al. attained the value semi-theoretically from the numerical analysis of the distribution of

stress-intensity factor around a crack using FEM method with the empirical data of the crack length and the diagonal size of silicon nitride ceramics indented at 196 N. Anstis et al. determined the value so that K_R calculated from the crack length fits to K_{Ic} from other conventional testing methods. Ramachandran et al. used the theoretical value derived from the analysis with the constant force model by Shetty et al.[16] In the Niihara's equation, $n = 2/5$, the value of which originated from the data fitting by Evans and Charles.[17] The value for ξ is 0.0309, which was also derived from the correlation analysis of the surface crack length and the fracture toughness obtained by other methods such as double-torsion technique.

In order to clarify the effect of crack length on the fracture resistance, indentation-strength-in-bending method, which can reveal the behavior in the longer-crack-length region, was also used. When a far-field stress is applied, the indentation cracks can be stably propagated to the instability crack length, c_T. Then the *R*-curve can be also determined as follows:[14]

$$K_R = \xi\left(\frac{E}{H}\right)^{1/2} P c_T^{-3/2} + \sigma Y c_T^{1/2} \quad (2)$$

where Y is a dimensionless configuration coefficient and σ is the fracture stress. In this study, Ramachandran's[7] and Braun's equations[18] were adopted for the sake of comparison. The values for ξ and Y in the Ramachandran's equation are 0.023 (the same as the Ramachandran's IF equation) and ~1.0, respectively, while those in the Braun's equation are 0.016 (the same as the Anstis's IF equation) and 0.77, respectively. In this study, the crack lengths at instability were estimated as 2.52 times larger than the lengths of as-indented surface cracks, since the c_T/c_0 measured experimentally for silicon nitride ceramics ranged from 2.2 to 2.5 as described by Ohji et al.[13] and 2.26 ± 0.18 in Ramachandran's paper,[7] which were close to the theoretical prediction of 2.52 for the constant point force model.[16]

3. Results

Table 1 shows the bulk densities for the three Si_3N_4. The relative densities of these samples were above 98.2%, indicating that these ceramics were almost fully densified. Fig. 1 shows the microstructures of the samples. It can be seen that 1A1Y sample consists of fine grains, whereas the grain size of 5A5Y sample (1950 °C/2 h) is larger than that of 1A1Y sample. After sintering 5A5Y at 1950 °C for 8 h, the grains grew further and elongated grains existed occasionally. In order to characterize these microstructural features quantitatively, the distributions of grain size for those samples were measured. The results of the grain size measurements are shown in Fig. 2. The range of grain diameters for 1A1Y sample was about 0.05–1.0 μm, whereas that for both of the 5A5Y samples were about 0.2–5 μm, which showed that the distributions of the grain diameter of both 5A5Y samples were about five times higher than that of 1A1Y. In the graph of 5A5Y sintered for 8 h, the fraction of small grains decreased, while that of larger ones increased, leading to a flat distribution of grain size. Correspondingly, the median grain diameter of 5A5Y (1950 °C/8 h) was 0.91 μm, which was ~3 times higher than that of 1A1Y (0.35 μm). The aspect ratio of

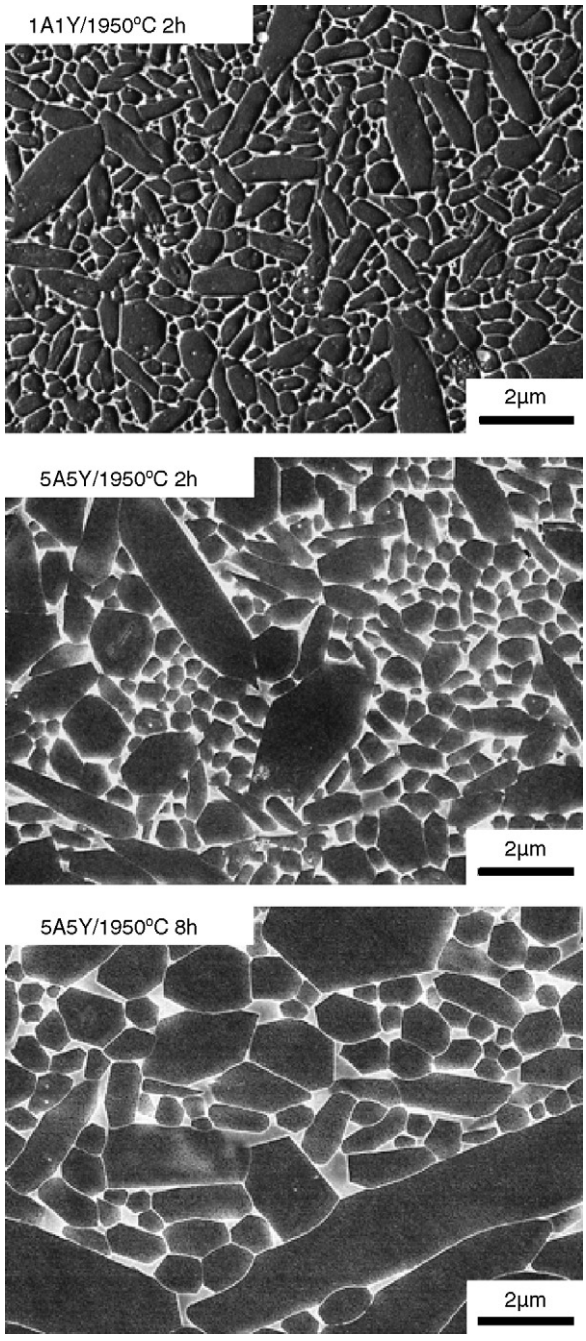

Fig. 1. SEM micrographs of the Si_3N_4 sintered with 1 wt% Al_2O_3/1 wt% Y_2O_3 at 1950 °C for 2 h, 5 wt% Al_2O_3/5 wt% Y_2O_3 at 1950 °C for 2 h and 5 wt% Al_2O_3/5 wt% Y_2O_3 at 1950 °C for 8 h.

Table 1
Bulk density, median grain diameter and aspect ratio of Si_3N_4 synthesized with different conditions

Property	1A1Y (1950 °C/2 h)	5A5Y (1950 °C/2 h)	5A5Y (1950 °C/8 h)
Bulk density (g cm^{-3})	3.19	3.22	3.22
Median grain diameter (μm)	0.35	0.52	0.91
Aspect ratio	4.1	4.9	5.5

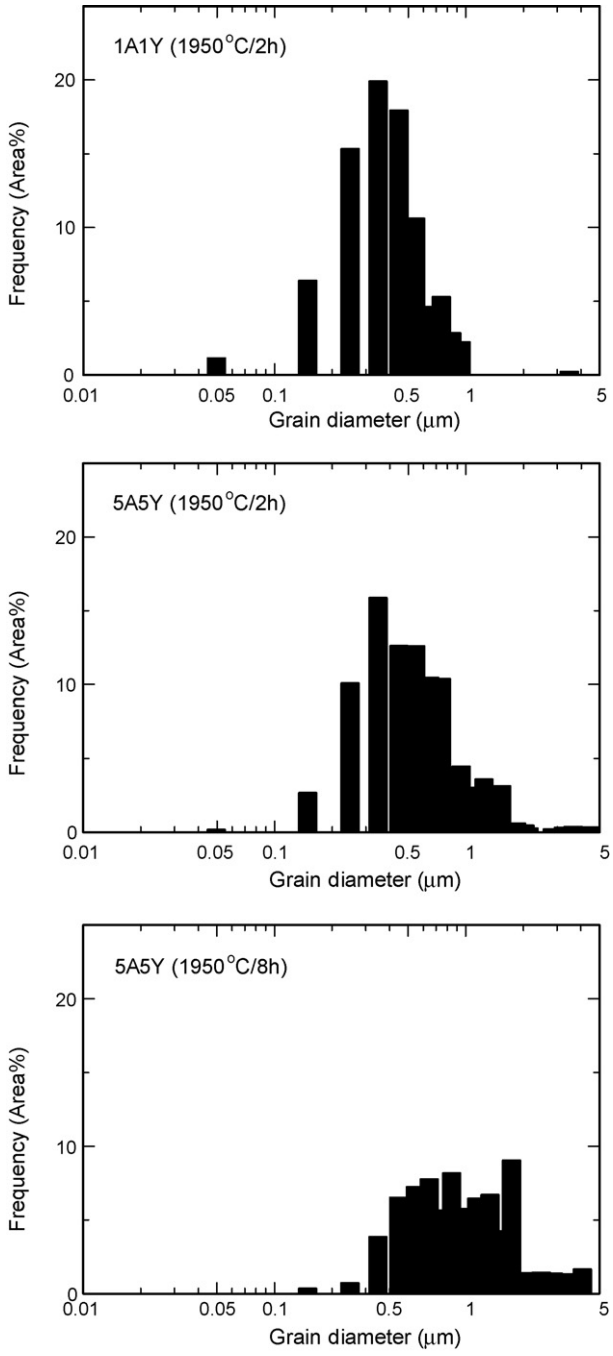

Fig. 2. Distributions of grain diameter for 1A1Y sample (1950 °C/2 h), 5A5Y sample (1950 °C/2 h) and 5A5Y sample (1950 °C/8 h).

the grains in 1A1Y was ∼4 and those of the grains in the 5 and 10k magnification images of 5A5Y samples sintered for 2 and 8 h were ∼5, whereas those of the coarse grains selected from the micrographs of ×1k were ∼10 for both 5A5Y samples, indicating that the limited number of grains have grown unidirectionaly.

Table 2 summarizes the mechanical data for the samples. The fracture toughness of 5A5Y (1950 °C/8 h) measured by the SEPB method was significantly higher than that of the 1A1Y sample, while that of 5A5Y sintered for 2 h showed the intermediate value. By contrast, the Young's modulus and the hardness

Table 2
Mechanical properties of Si_3N_4 with different microstructures

Property	1A1Y (1950 °C/2 h)	5A5Y (1950 °C/2 h)	5A5Y (1950 °C/8 h)
Young's modulus (GPa)	315	300	306
Vickers hardness (GPa)[a]	15.4	14.3	13.9
Fracture toughness (MPa m$^{1/2}$)	4.5 ± 0.1	6.9 ± 0.1	8.3 ± 0.2

[a] The indentation load was 196 N.

for 5A5Y (1950 °C/8 h) was slightly lower than those for the 1A1Y sample. This was attributed to the increase in the volume fraction of grain boundary phases which were softer than pure silicon nitride. The remarkable difference in the fracture toughness among samples seems to originate from the difference in the morphology of the grains since both the Young's modulus and hardness did not vary significantly.

The IF equations used in this study require that the crack pattern be well developed and the literatures specify the valid range as the ratio of as-indented crack length to the half of the diagonal of the "plastic" impression, c_0/a. The Niihara's equation demands c_0/a be over ∼2.5 and those of Anstis and Ramachandran require $c_0/a > 2$. Although there is no description of the suitable range of the ratio in Miyoshi's paper, their FEM calculations were based on the empirical data of both c_0 and a at 196 N and $c_0/a = 2$. Therefore a critical value of 2 was also used for the case of the Miyoshi's equation. For 1A1Y material, c_0/a was larger than 2.5 in the range of the load investigated, confirming that the cracks were median-radial cracks.[5] Thus, all the four equations can be used for assessing the fracture toughness of 1A1Y. In the case of 5A5Y samples (1950 °C/2 h), the condition of $c_0/a > 2.5$ was satisfied only in the load range of 294–490 N, and the ratios for the loads of 49–196 N were $2.0 < c/a < 2.5$. Three equations, Anstis's, Ramachandran's and Miyoshi's equations, were applicable for all loads, while Niihara's equation was only valid at the load of 294 and 490 N. In the case of 5A5Y samples sintered for 8 h, the ratio of c_0/a was over 2.5 only at the load of 490 N and the ratios for the lower loads were $2.0 < c_0/a < 2.5$. The Niihara's equation was only valid at the load of 490 N, while the rest of the equations were applicable for all loads. However, Niihara suggested that the critical ratio of 2.5 for transition from the Palmqvist to the median cracks was worthy of further research.[19] Lube investigated the crack system of silicon nitride ceramics indented at various loads using the serial sectioning technique and showed that the crack pattern at a load of 98 N was the half-penny type although $c_0/a = 2.2$ and the pattern at 49N was half-penny type in some cases regardless of the low c_0/a of 1.8.[20] Our previous study concerning the crack profiles of the indentations in this study also identified the crack types as half-penny rather than the Palmqvist type.[21] The Niihara's equation was therefore also applied to the indentations of 5A5Y samples at lower loads since the equation was developed for the median/radial (half-penny) cracks.

The fracture resistances determined from the as-indented crack lengths are shown in Figs. 3–5, as a function of the

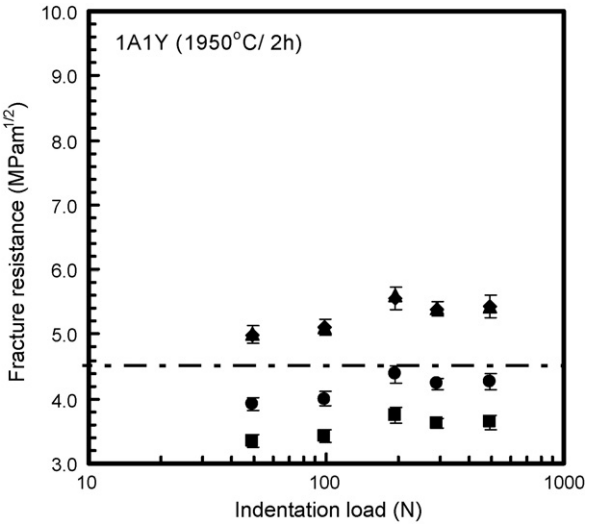

Fig. 3. Dependence of fracture resistance of 1A1Y sample (1950 °C/2 h) on the indentation loads determined by IF method with equations of Miyoshi (●), Anstis (■), Ramachandran (▲) and Niihara (♦). Dashed and single-dotted line shows fracture toughness from SEPB.

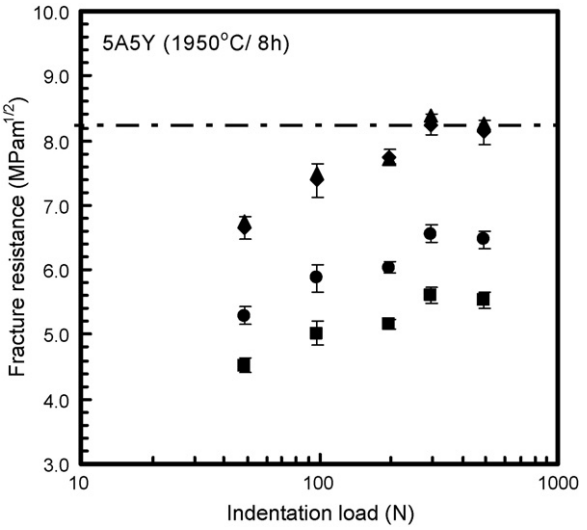

Fig. 5. Dependence of fracture resistance of 5A5Y sample (1950 °C/8 h) on the indentation loads determined by IF method with equations of Miyoshi (●), Anstis (■), Ramachandran (▲) and Niihara (♦). Dashed and single-dotted line shows fracture toughness from SEPB.

indentation load. The fracture resistances of 1A1Y sample calculated with the Niihara's and the Ramachandran's equations were almost the same and were apparently larger than the value from the SPBP method at any indentation load. By contrast, the fracture resistance from the Anstis's equation showed a much smaller value than the fracture toughness from SEPB at the low indentation loads and increased slightly with increasing load. However, it did not reach the K_{Ic} from SEPB. K_R from Miyoshi's equation at the low loads was smaller than K_{Ic} from SEPB and increased with increasing the load to become closest to K_{Ic}.

In the case of 5A5Y sintered for 2 h (Fig. 4), the fracture resistances estimated from the Miyoshi and Anstis equations at the low load were far below the fracture toughness from SEPB and increased with the load but did not reach K_{Ic}. K_R from Niihara's and Ramachandran's equations showed the same values again and were almost equal to K_{Ic} from SEPB at 49 N. In the case of 5A5Y sintered for 8 h (Fig. 5), all of the fracture resistances estimated from the four equations at the low load were far below K_{Ic} from SEPB and increased with the load. Among the four equations, the estimation with the Niihara's and the Ramachandran's equations at loads over 294 N gave the nearest value to K_{Ic}, while the estimation with the Anstis's equation showed a large discrepancy even at the highest load. It is obvious that the determination of the most reliable equation from these limited data is difficult since the equation which gave the nearest value

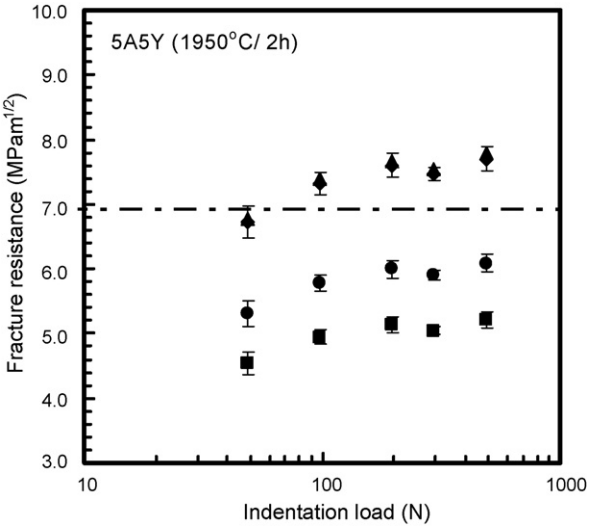

Fig. 4. Dependence of fracture resistance of 5A5Y sample (1950 °C/2 h) on the indentation loads determined by IF method with equations of Miyoshi (●), Anstis (■), Ramachandran (▲) and Niihara (♦). Dashed and single-dotted line shows fracture toughness from SEPB.

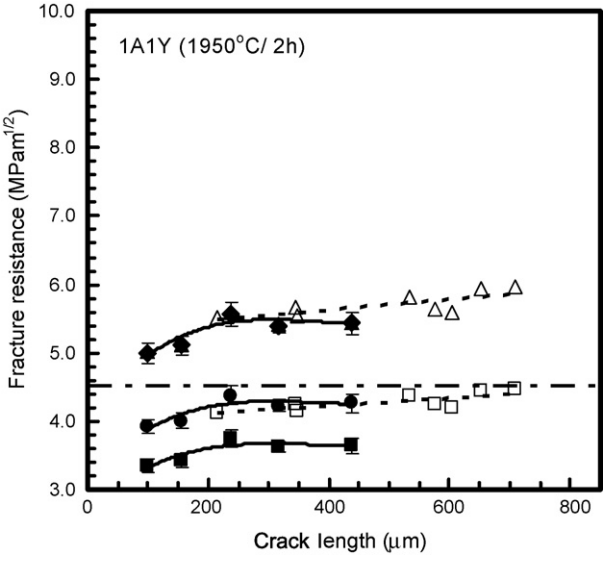

Fig. 6. Fracture resistance vs. crack length for 1A1Y sample (1950 °C/2 h) determined by as-indented crack lengths (closed symbols) and instability crack lengths (open symbols). (●) Miyoshi; (■) Anstis; (▲ and △) Ramachandran; (♦) Niihara; (□) Braun. Dashed and single-dotted line shows fracture toughness from SEPB.

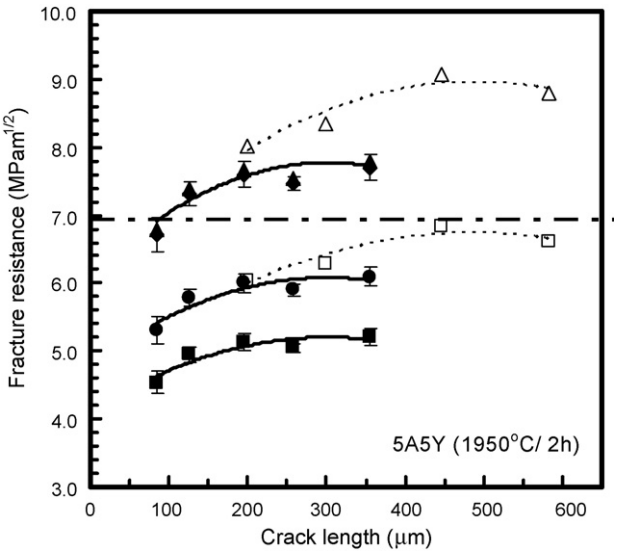

Fig. 7. Fracture resistance vs. crack length for 5A5Y sample (1950 °C/2 h) determined by as-indented crack lengths (closed symbols) and instability crack lengths (open symbols). (●) Miyoshi; (■) Anstis; (▲ and △) Ramachandran; (♦) Niihara; (□) Braun. Dashed and single-dotted line shows fracture toughness from SEPB.

to the toughness from SEPB was different depending on the microstructure of Si_3N_4 ceramics.

The *R*-curve behavior is known to appear in the so called self-reinforced Si_3N_4 which consists of large elongated grains.[22,23] It is rational to expect that the increments in the fracture resistance with the indentation load in Figs. 3–5 are interpreted as the effect of the *R*-curve behavior. Figs. 6–8 show the dependence of the calculated fracture resistance on the crack length (closed symbols). The plots of the fracture resistance from the four equations revealed the rising *R*-curve behavior in both 5A5Y samples,

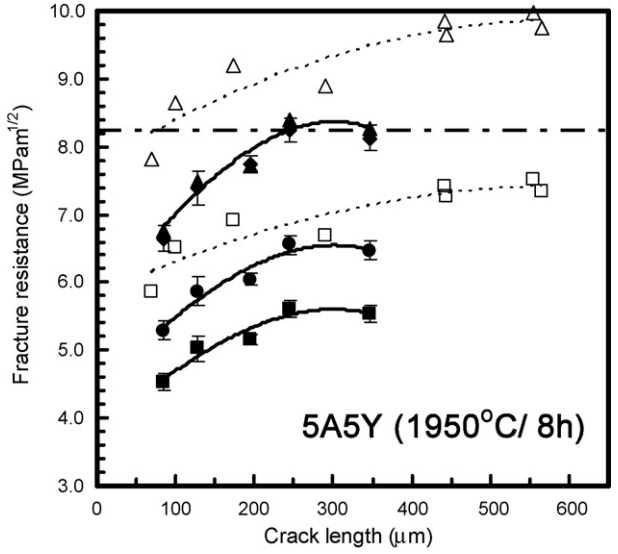

Fig. 8. Fracture resistance vs. crack length for 5A5Y sample (1950 °C/8 h) determined by as-indented crack lengths (closed symbols) and instability crack lengths (open symbols). (●) Miyoshi; (■) Anstis; (▲ and △) Ramachandran; (♦) Niihara; (□) Braun. Dashed and single-dotted line shows fracture toughness from SEPB.

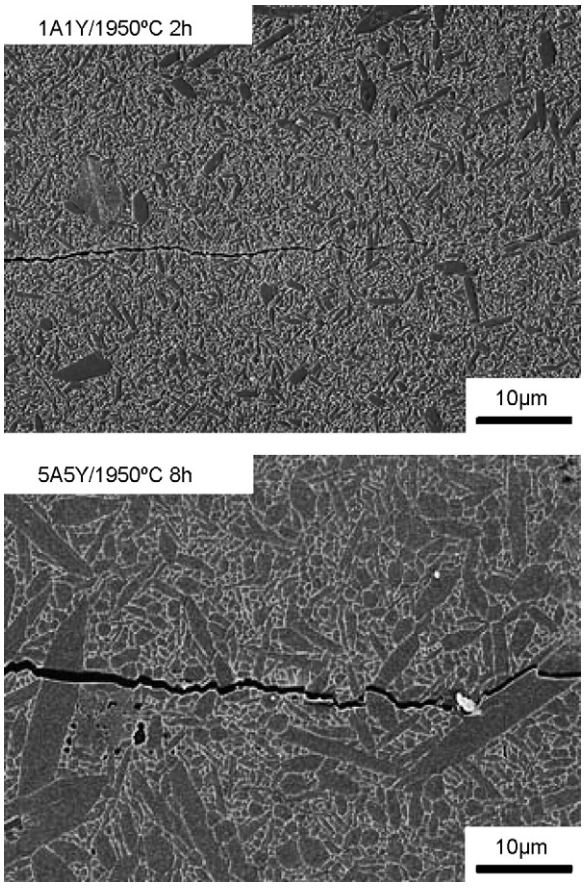

Fig. 9. Propagation of crack generated by indentation in 1A1Y sample (1950 °C/2 h) and 5A5Y sample (1950 °C/8 h). The indentation load was 196 N.

while a small increase in fracture resistance was observed in the 1A1Y sample. Since the range of as-indented crack length was limited, it is difficult to deduce whether the value obtained by IF techniques at highest load saturated or not.

In order to clarify the *R*-curve behavior in the longer crack-length region, the fracture resistances attained from the ISB method are also plotted on Figs. 6–8 (open symbols). In Fig. 6 (1A1Y), the plot of the ISB data from the Braun's equation (open squares) started from the point near-by the Miyoshi's data at higher load and continued to increase slightly with increasing the load toward the value from SEPB. The ISB data from the Ramachandran's equation also increased slightly with the crack length, ensuring the almost flat *R*-curve behavior of this material.

In the case of both 5A5Y samples sintered for 2 and 8 h (Figs. 7 and 8), the series of ISB data from the Braun's equation rose significantly with crack length. The ISB data from the Ramachandran's equation also showed the apparent rising behavior. Thus, the *R*-curve behavior was also confirmed in the wider region of crack length (about 100–600 μm), as well as the shorter range studied by the IF method.

4. Discussion

The enhancement in the fracture toughness of the silicon nitride with elongated grains has been reported by several

researchers[24–26] and its mechanism was generally accepted as the effect of shielding force caused by the bridging of elongated grains in the crack wake.[22,23] In order to verify whether this explanation is valid for the results of this study, the propagation of the cracks was observed with SEM. Fig. 9 shows the comparison of the propagation of the cracks in 1A1Y and 5A5Y sintered for 8 h. The pullout of the grains and crack deflection occurred in 5A5Y (1950 °C/8 h) sample, whereas such phenomena were seldom observed and the crack extended straightforward in the 1A1Y sample. Therefore, the origin of the enhanced fracture toughness of 5A5Y sample can be explained by the mechanism of crack bridging of the elongated grains. It is reasonable to suppose that the *R*-curve behavior observed in both 5A5Y samples is attributable to the same mechanism as well.

From the theoretical point of view, the fracture toughness, K_{Ic}, obtained by the SEPB may differ from the fracture resistance, K_R, obtained by IF technique since K_{Ic} is for fast crack propagation, whereas K_R is for crack arrest. Then, the comparison of K_R with K_{Ic} is not significant in the academic field, while it makes sense in the engineering field as described above. Accordingly, the comparison of K_{Ic} from SEPB and K_R from IF method has been conducted by several researchers. In the case of the silicon nitride with the flat *R*-curve behavior, Awaji et al.[10,11] and Pezzotti et al.[27] examined the validity of K_R determinations by various techniques using Si_3N_4 ceramics with relatively low fracture toughness, 2–5 MPa $m^{1/2}$. They pointed out that the fracture resistance estimated by the Niihara's equation was higher than the fracture toughness from SEPB technique. Awaji et al.[10,11] also reported that K_R from the Miyoshi's equation at the load over 98 N was relatively close to K_{Ic} from SEPB, which is consistent with our results. Also, the roughly estimated K_R with Miyoshi's equation using the data of Pezzotti (by multiplying the K_R from the Niihara's equation with an appropriate constant), exhibited a coincidence with the value obtained from the other techniques. The consistency between K_R from the Miyoshi's equation and K_{Ic} from SEPB was also verified for Al_2O_3, SiC and Si_3N_4 by the round-robin test conducted to standardize the toughness testing method,[28] which allowed the adoption of IF method as standard test technique in the JIS R1607.

The closest outcome using Miyoshi's equation seems to be caused by the fact that the parameter *n* was estimated from the quasi-theoretical analysis using FEM method with the measured values of crack length and diagonal size of Si_3N_4 indented at 196 N. By contrast, the value of *n* for the Ramachandran's equation came from the approximation using the simplified model. It is reasonable to expect that the accuracy of the estimation from such approximation should be inferior to that of Miyoshi's estimation. In the case of the Anstis's and Niihara's equations, the values of *n* were the average using a host of miscellaneous materials such as glasses, Al_2O_3, B_4C and Si_3N_4, etc. The difficulty in detecting the crack tips and the amount of post-indentation slow crack growth differ among these materials,[10,11] which would result in the inadequate values of *n* for Si_3N_4 ceramics. Thus, in the case of the Si_3N_4 with the almost flat *R*-curve behavior, good agreement between the K_R from IF techniques and K_{Ic} from SEPB seems to be obtained generally when the Miyoshi's equation was adopted at the higher indentation load.

For the Si_3N_4 with the rising *R*-curve behavior, the discrepancy between K_R obtained by the IF and K_{Ic} from SEPB techniques was reported by Choi and Salem[29] and Yang et al.[30] Choi and Salem reported that K_{Ic} of the in situ-toughened Si_3N_4 determined by the SEPB method was ~10 MPa $m^{1/2}$, while K_R by the IF method with the Anstis's formula at the load of 49–294 was ~6 MPa $m^{1/2}$. Almost the similar difference between K_R and K_{Ic} from the Anstis's equation at the same range of loads was attained in our study for 5A5Y (1950 °C/8 h) sample, which is attributable to the resembling microstructures. However, the discrepancy was reduced to ~2 MPa $m^{1/2}$ in the case of 5A5Y sample sintered for 2 h, indicating that the relation between the two values depends on the microstructure. Yang et al. investigated the mechanical properties of Si_3N_4 with different microstructures and showed that most of K_R from the Niihara's equation at the load of 200 N showed 6–7 MPa $m^{1/2}$, which were smaller than K_{Ic} from SEPB method (7–10 MPa $m^{1/2}$). They also reported that K_{Ic} from SEPB decreased significantly with increasing the amount of additives while K_R from IF decreased slightly, resulting in the opposite relation for the sample sintered using the largest amount of additives. The same tendency was also observed in our study; K_{Ic} from SEPB increased from 6.9 to 8.3 MPa $m^{1/2}$ with increasing the sintering time, whereas the change in K_R from the Niihara's equation at 196 N was negligible (7.6–7.8 MPa $m^{1/2}$). Therefore, it is reasonable to conclude that the relation between the two values is affected by the microstructures.

Choi and Salem[29] and Yang et al.[30] attributed the smaller values from the IF method to the rising *R*-curve behavior of the materials; IF technique gave the K_R at the short crack size, whereas SEPB technique gave the value at the longer size (1–2 mm). If this was the case, the fracture resistance obtained from IF data would be smaller than the K_{Ic} from SEPB in the whole range of crack length investigated, leading to the conclusion that the Niihara's equation overestimated the fracture resistance. However, Nose et al. reported that the process zone wake in alumina did not affect the K_{Ic} values evaluated by the SEPB technique, indicating that the length of the precrack did not correspond to the crack length in the plot of K_{Ic} versus crack extension.[2] This phenomenon is explained as follows: due to the rapid pre-crack development in the SEPB method, bridge formation by elongated grains is limited, leading to the situation where the pop-in crack remain free from shielding force operating in the crack wake. Although the effective crack length for SEPB test has been estimated using coarse alumina[31] and a Si_3N_4–SiC platelet composite[27] both of which showed the rising *R*-curve behavior, there have been few reports that investigate the effective crack length for SEPB using Si_3N_4. Then we can not deny, at this stage, the possibility of the situation that the SEPB's effective crack length is increased by the coarsening of the microstructure of the sample, which gives the reasonable explanation for the relation of the K_{Ic} from SEPB and K_R from IF with Niihara's equation mentioned above. Therefore, it is necessary to clarify the effective crack extension of the SEPB test when K_{Ic} of Si_3N_4 with rising *R*-curve behavior is evaluated and compared with K_R from IF methods.

5. Conclusions

In order to clarify the suitable IF formula for the practical assessment of fracture resistance needed in the markets of small ceramic parts, three types of silicon nitride ceramics were fabricated, one with fine and uniform structure and the others with coarse and elongated structure, and their fracture resistance was evaluated using the IF method with various indentation loads ranging from 49 to 490 N. The plots of fracture resistance versus the as-indented crack length as well as the instability crack length revealed the *R*-curve behavior for both coarse silicon nitrides and flat *R*-curve for the fine silicon nitrides. By comparing the fracture toughness, K_{Ic}, estimated from the SEPB and the fracture resistance, K_R, from IF using four different equations, an agreement between the K_{Ic} and K_R was observed for the silicon nitrides with fine structure by applying the Miyoshi's equation to the indentations at the load above 196 N. By contrast, K_R of the coarse silicon nitrides from the equations of Niihara and Ramachandran coincided with K_{Ic} at the different indentation load depending on the microstructures. When the *R*-curve behavior was negligible, our results were consistent with the previous reports, indicating that Miyoshi's equation at the high indentation load is universally preferable for silicon nitrides with the fine and uniform microstructure. By contrast, in the case of the rising *R*-curve behavior, the situation was complicated due to the uncertainties of the effective crack length for SEPB test, which suggest the necessity of further investigation on the effect of precrack length on K_{Ic} when the best IF equation for coarse silicon nitride samples is to be selected on the basis of comparability with the SEPB.

Acknowledgment

This work has been supported by METI, Japan, as part of the international standardization project of test methods for rolling contact fatigue and fracture resistance of ceramics for ball bearings.

References

1. Lawn, B. R., Evans, A. G. and Marshall, B., Elastic/plastic indentation damage in ceramics: the median/radial crack system. *J. Am. Ceram. Soc.*, 1980, **63**, 574–581.
2. Nose, T. and Fujii, T., Evaluation of fracture toughness for ceramic materials by a single-edge-precracked-beam method. *J. Am. Ceram. Soc.*, 1988, **71**, 328–333.
3. *Testing Methods for Fracture Toughness of Fine Ceramics*. Japanese Industrial Standard, JIS R 1607, 1995.
4. Miyoshi, T., Sagawa, N. and Sasa, T., Study of evaluation for fracture toughness of structural ceramics. *J. Jpn. Soc. Mech. Eng. A*, 1985, **51**, 2489–2497.
5. Niihara, K., Morena, R. and Hasselman, D. P. H., Evaluation of K_{Ic} of brittle solids by the indentation method with low crack-to-indent ratios. *J. Mater. Sci. Lett.*, 1982, **1**, 13–16.
6. Anstis, G. R., Chantikul, P., Lawn, B. R. and Marshall, D. B., A critical evaluation of indentation techniques for measuring fracture toughness. I. Direct crack measurements. *J. Am. Ceram. Soc.*, 1981, **64**, 533–538.
7. Ramachandran, N. and Shetty, D. K., Rising crack-growth-resistance (*R*-curve) behavior of toughened alumina and silicon nitride. *J. Am. Ceram. Soc.*, 1991, **74**, 2634–2641.
8. Ponton, C. B. and Rawlings, R. D., Vickers indentation fracture toughness test. Part 1. Review of literature and formulation of standardized indentation toughness equations. *Mater. Sci. Tech.*, 1989, **5**, 865–872.
9. Ponton, C. B. and Rawlings, R. D., Vickers indentation fracture toughness test. Part 2. Application and critical evaluation of standardized indentation toughness equations. *Mater. Sci. Tech.*, 1989, **5**, 961–976.
10. Awaji, H., Yamada, T. and Okuda, H., Results of the fracture toughness test round robin on ceramics—VAMAS project. *J. Ceram. Soc. Jpn.*, 1991, **99**, 417–422.
11. Awaji, H., Kon, J. and Okuda, H., The VAMAS hardness round robin on ceramic materials. *VAMAS Report #9*. Japan Fine Ceramic Center, Nagoya, 1990.
12. Rossignol, F., Goursat, P. and Besson, J. L., Microstructue and mechanical behavior of self-reinforced Si_3N_4 and Si_3N_4–SiC whisker composites. *J. Eur. Soc. Ceram.*, 1994, **13**, 299–312.
13. Ohji, T., Hirao, K. and Kanzaki, S., Fracture resistance behavior of highly anisotoropic silicon nitride. *J. Am. Ceram. Soc.*, 1995, **78**, 3125–3128.
14. Chantikul, P., Anstis, G. R., Lawn, B. R. and Marshall, D. B., A critical evaluation of indentation techniques for measuring fracture toughness. II. Strength method. *J. Am. Ceram. Soc.*, 1981, **64**, 539–543.
15. Mitomo, M., Tsutsumi, M. and Tanaka, H., Grain growth during gas-pressure sintering of β-silicon nitride. *J. Am. Ceram. Soc.*, 1990, **73**, 2441–2445.
16. Shetty, D. K., Rosenfield, A. R. and Duckworth, W., Analysis of indentation crack as a wedge-loaded half penny crack. *J. Am. Ceram. Soc.*, 1985, **68**, C65–C67.
17. Evans, A. G. and Charles, E. A., Fracture toughness determination by indentation. *J. Am. Ceram. Soc.*, 1976, **59**, 371–372.
18. Braun, L. M., Bennsion, S. J. and Lawn, B. R., Objective evaluation of short-crack toughness curves using indentation flaws: case study on alumina-based ceramics. *J. Am. Ceram. Soc.*, 1992, **75**, 3049–3057.
19. Niihara, K., Morena, R. and Hasselman, D. P. H., Further reply to comment on elastic/plastic indentation damage in ceramics: the median/radial crack system. *J. Am. Ceram. Soc.*, 1982, **65**, C116.
20. Lube, T., Indentation crack profiles in silicon nitride. *J. Eur. Ceram. Soc.*, 2001, **21**, 211–218.
21. Miyazaki, H., Hyuga, H., Hirao, K. and Ohji, T., in preparation.
22. Becher, P. F., Microstructural design of toughened ceramics. *J. Am. Ceram. Soc.*, 1991, **74**, 255–269.
23. Steinbrech, R. W., Toughening mechanisms for ceramic materials. *J. Eur. Ceram. Soc.*, 1992, **10**, 131–142.
24. Tani, E., Umebayashi, S., Kishi, K., Kobayashi, K. and Nishijima, M., Gas-pressure sintering of Si_3N_4 with concurrent addition of Al_2O_3 and 5 wt% rare earth oxide: high fracture toughness with fiber-like structure. *Am. Ceram. Soc. Bull.*, 1986, **65**, 1311–1315.
25. Kawashima, T., Okamoto, H., Yamamoto, H. and Kitamura, A., Grain size dependence of the fracture toughness of silicon nitride ceramics. *J. Ceram. Soc. Jpn.*, 1991, **99**, 320–323.
26. Hirosaki, N., Akimune, Y. and Mitomo, M., Effect of grain growth of β-silicon nitride on strength, Weibull modulus, and fracture toughness. *J. Am. Ceram. Soc.*, 1993, **76**, 1892–1894.
27. Pezzotti, G., Niihara, K. and Nishida, T., Some microstructural conditions for evaluating fracture toughness and *R*-curve behavior in platelet-reinforced composites. *J. Test Eval.*, 1993, **21**, 358–365.
28. *Report of Preliminary Investigation for Standardization of Fine Ceramics*. Japanese Fine Ceramics Association, 1998.
29. Choi, S. R. and Salem, J. A., Crack-growth resistance of in situ-toughened silicon nitride. *J. Am. Ceram. Soc.*, 1994, **77**, 1042–1046.
30. Yang, J., Sekino, T. and Niihara, K., Effect of grain growth and measurement on fracture toughness of silicon nitride ceramics. *J. Mater. Sci.*, 1999, **34**, 5543–5548.
31. Nishida, T. and Kameyama, I., Evaluation of fracture toughness for structural ceramics using SEPB specimens (part 4). *J. Ceram. Soc. Jpn.*, 1992, **100**, 276–281.